

Optimization of the Distribution of Green Buildings Based on Urban Heat Island Effect

Guoshuai Zhong, Wenxuan Wang*

College of water Resources and Civil Engineering, Hunan Agriculture University, Changsha 410128, China

Corresponding Author Email: wangwenxuan1221@hunau.edu.cn



<https://doi.org/10.18280/ijht.400140>

ABSTRACT

Received: 3 October 2021

Accepted: 8 December 2021

Keywords:

urban heat island (UHI) effect, green building, distribution, optimization

Green buildings are an important constituent part of the urban ecosystem; they act as an adjuster of temperature and humidity of the environment in cities, and can effectively alleviate the Urban Heat Island (UHI) effect. Existing studies on the UHI effect generally ignored the local information in the changes of the UHI effect, and the impact of the optimization of green building distribution on the UHI effect hadn't been taken into consideration. To fill in this research gap, this paper aims to study the optimization of the distribution of green buildings based on the UHI effect. At first, this paper adopted a high-precision radiative transfer model to invert the temperature of earth surface in cities, and accurately calculate the UHI effect. Then, this paper analyzed the changes in the UHI effect caused by the optimization of the distribution of green buildings and the response of human activities, and used the time variation law of the single pixels of green buildings to reflect the spatial variation law of the UHI effect. At last, experimental results gave the optimization results of the distribution of green buildings based on the UHI effect.

1. INTRODUCTION

The fast growth of urban population makes the coverage area of urban buildings to expand continuously, and the underlying earth surface of the cities has become increasingly diversified, which has resulted in the UHI effect that can change the climate in cities [1-6]. The adverse impact of the UHI effect includes high temperature in urban areas, deterioration of natural environment [7-14], and damages to the physical health of urban residents. Therefore, mitigating the UHI effect is a common requirement for improving eco-environment quality and ensuring the health of residents [15-16]. Green buildings are in accord with the sustainable development goal of cities, they are an important constituent part of the urban ecosystem [17-22]; they act as an adjuster of temperature and humidity of the environment in cities, and can effectively alleviate the UHI effect [23-27]. Thus, researching the evolution law of the distribution of green buildings via analyzing the UHI effect is of great practical value.

UHI effect is a global threat to the energy demand of urban buildings, the public health, and the energy security. To solve this problem, world scholars have conducted various studies, for example, Susca et al. [28] discussed the impact of the deployment of green walls under different conditions of cooling/warming season, weather, day/night time, wall direction, and application scale. At present, cities are generally facing the dual threats of global warming and UHI effect, and the urban buildings are both the cause and the victim of overheating in cities. He [29] proposed the a GB-based UHIM system and the concepts of "Zero UHI effect buildings", "Zero heat buildings", and "Neutral microclimate buildings", and the goal was to remove excess heat and achieve zero thermal impact on the surrounding environment through reasonable architecture design and operation and applying new technologies based on the BG goals. To figure out the impact

of vegetation on thermal environment, Sun et al. [30] collected temperature data from a green roof and a common roof of a same office building and analyzed the impact of vegetation on thermal environment, and their research results showed that the maximum cooling effect of the green roof in summer was -1.60°C and -0.26°C on average. Modern green buildings tend to pay more attention to the indoor space environment and have different requirements for health, comfort and user productivity. Generally speaking, green buildings can make full use of the sunlight and save energy. Wang and Mao [31] proposed a method for simulating vertical temperature distribution in green buildings based on the niche genetic algorithm, they adopted the idea of niche to reflect the sharing function of similarity between individuals based on the sharing mechanism, so as to obtain the spatial fitness degree of each layer; then they calculated the temperature and internal force of the connecting members and the internal and external vertical members, and the vertical temperature distribution in green buildings. Tong [32] proposed to use an index of distribution (IOD) to describe the distribution pattern of buildings in green space; with Nanjing Yuhuatai Park and Qingliangshan Park as examples, the effectiveness of IOD had been verified; the paper also constructed a model based on genetic algorithm, which can generate building plans corresponding to specific IODs.

Existing studies generally focus on the inversion and calculation of the distribution of green buildings based on remote sensing images, they tend to take manual labeling as the basis, while ignoring the local information in the changes of the UHI effect, and they haven't considered the impact of the optimization of green building distribution on the UHI effect. For this reason, this paper studied the optimization of the distribution of green buildings in cities based on an analysis of the UHI effect. The main content of this paper includes these aspects: the second chapter adopted a high-

precision radiative transfer model to invert the temperature of earth surface in cities and calculate the UHI effect accurately; the third chapter analyzed the changes in the UHI effect caused by the optimization of the distribution of green buildings and the response of human activities, and used the time variation law of the single pixels of green buildings to reflect the spatial variation law of the UHI effect. At last, experimental results gave the optimization results of the distribution of green buildings based on the UHI effect.

2. ANALYSIS OF THE UHI EFFECT

In order to accurately calculate the UHI effect, this paper chose to use a high-precision radiative transfer model to invert the temperature of earth surface in the city. At First, the thermal radiation effect of the atmosphere on the urban earth surface was evaluated, then, this effect was eliminated, and the temperature of urban earth surface was estimated again. Assuming: $HF(\Gamma)$ represents the black-body radiation at temperature Γ ; K_μ represents the thermal infrared radiation; K_{up} and K_{down} represent the up-flow and down-flow; ρ represents the transmissivity of the thermal infrared band; σ represents the earth surface irradiance, then there are:

$$HF(\Gamma) = (K_\mu - K_p - \rho \times (1 - \sigma) \times K_D) / (\rho \times \sigma) \quad (1)$$

$$\Gamma = L_2 / \ln(L_1 / HF(\Gamma)) + 1 \quad (2)$$

The value of σ was estimated using the threshold method based on the different building types and land utilization types. Assuming: E_H , E_Y , and E_Z respectively represent green space, ordinary buildings, and green buildings; σ_m , σ_x , σ_H , σ_R , and σ_Z respectively represent the surface radiance of traditional urban earth surface, optimized urban earth surface, green space, ordinary buildings, and green buildings, then there are:

$$\sigma_m = T_H E_H \sigma_H + (1 - T_H) E_Y \sigma_Y + d\sigma \quad (3)$$

$$\sigma_x = T_H E_H \sigma_H + (1 - T_H) E_Z \sigma_Z + d\sigma \quad (4)$$

The values of σ_H , σ_R , and σ_Z could be assigned by referring to the proportions of the areas of green space, ordinary buildings and green buildings in the total area of urban earth surface, then the values of E_H , E_Y , and E_Z could be calculated further. After that, by estimating the maximum and minimum values of the green building coverage index (GBC_{max} and GBC_{min}) in each labeled thermal infrared image of the city, the value of T_H could be calculated:

$$T_H = \left[\frac{GBC - GBC_{min}}{GBC_{max} - GBC_{min}} \right]^2 \quad (5)$$

In order to accurately measure the changes in the UHI effect before and after the optimization of green building distribution, this paper chose to take the difference between ordinary buildings and green buildings as the indicator. Assuming: K_{SU} represents the UHI index; K_{UR} represents the temperature of green building pixels; K_{AV} represents the average temperature of earth surface of ordinary buildings; K_c represents the difference between the temperature of earth surface of

ordinary buildings and the temperature of earth surface of green buildings; K_{RU} represents the earth surface temperature of ordinary building pixels, then there are:

$$K_{SU} = K_{UR} - K_{AV} \quad (6)$$

$$K_c = K_{RU} - K_{AV} \quad (7)$$

The collected UHI index data were divided according to time periods. To verify the change trends of green building pixels in different time periods, based on the M-K test method which does not require samples to obey a defined distribution, this paper processed the change trends of the time series of the UHI index, the specific process is:

$$R = \sum_{i=1}^{m-1} \sum_{u=l+1}^m \text{sgn}(g_i - g_u) \quad (8)$$

Assuming: m represents the dataset length of the UHI index; g_i and g_u respectively represent the value of green building pixels at time moment i and time moment u ; the integer variables returned by the sgn function are 1, 0, and -1, respectively corresponding to the three situations of $g_i > g_u$, $g_i = g_u$, and $g_i < g_u$. When $R \geq 0$, the green building pixels are in an upward trend; when $R \leq 0$, the green building pixels are in a downward trend. If the number of data samples m exceeds 10, then the distribution is a normal distribution; moreover, in the paper, the 95% significance level has been selected as the standard, then the expectation QW , variance FC , and the standard normal system variable SN can be expressed as:

$$QW = 0 \quad (9)$$

$$FC = m(m-1)(2m+5)/18 \quad (10)$$

$$SN = \begin{cases} \frac{R-1}{\sqrt{FC}}, & R > 0 \\ 0, & R = 0 \\ \frac{R+1}{\sqrt{FC}}, & R < 0 \end{cases} \quad (11)$$

For all green building pixels with obvious change trends, this paper adopted the Theil-Sen Median trend analysis method to calculate the slope Ψ of the time series. When Ψ is greater than 0, the time series of the UHI index show an increasing trend; when Ψ is equal to 0, the trend of the time series of the UHI index is not obvious; when Ψ is less than 0, the time series of the UHI index show a decreasing trend. The calculation formula of Ψ is as follows:

$$\Psi = \Omega((g_i - g_u)/(i - u)), \forall i > u \quad (12)$$

According to the Jenks Natural Breaks Classification, the change trends of timer series of the UHI index were divided into 5 degrees, including fast decrease, slow decrease, basically unchanged, slow increase, and fast increase, as listed in Table 1. The shifting of the center of gravity of the UHI index data represents the changes in the urban thermal environment caused by the changes of the distribution of green

buildings in the city. Assuming N_i represents the weight; A_i and B_i represent the longitude and latitude coordinates of green building pixels; A_n and B_n represent the longitude and latitude coordinates of the center of gravity, then there are:

$$A_n = \frac{\sum_{i=1}^m N_i A_i}{\sum_{i=1}^m N_i} \quad (13)$$

$$B_n = \frac{\sum_{i=1}^m N_i B_i}{\sum_{i=1}^m N_i} \quad (14)$$

Figure 1 gives a few examples of the changes of gravity center of the UHI effect in the study area. To further get the increase or decrease direction of the UHI index data, this paper used the standard ellipse tool to analyze the data, that is, to

describe the direction based on the bias of the long axis of the ellipse. The axes of the ellipse can be determined by the standard deviations of the coordinates in the a and b directions relative to the center of the ellipse. Assuming: a_i and b_i represent the horizontal and vertical coordinates of sample point i of the UHI index data; m represents the total number of sample points of the UHI index data; A^* and B^* represent the average values of the horizontal and vertical coordinates of the sample points, then there are:

$$BIA_a = \sqrt{\frac{\sum_{i=1}^m (a_i - A^*)^2}{m}} \quad (15)$$

$$BIA_b = \sqrt{\frac{\sum_{i=1}^m (b_i - B^*)^2}{m}} \quad (16)$$

Table 1. Division criteria of change degrees

Degree	Fast decrease	Slow decrease	Basically unchanged	Slow increase	Fast increase
No. of degree	1	2	3	4	5
<i>M-K</i> Test	Lower than -2	Lower than -2	Higher than -2 and lower than 2	Higher than 2	Higher than 2

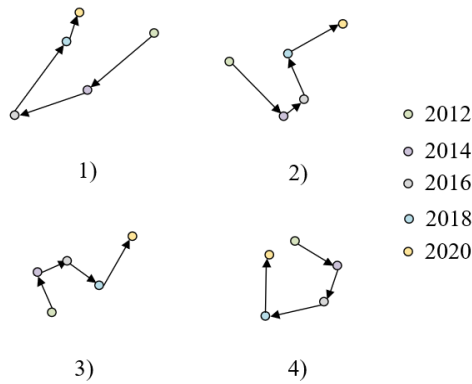


Figure 1. Changes of the center of gravity of the UHI effect in the study area

3. IMPACT OF THE OPTIMIZATION OF GREEN BUILDING DISTRIBUTION

This paper aims to analyze the impact of the optimization of the distribution of green buildings on the UHI effect and the response of human activities. In this paper, the time variation law of single green building pixels was adopted to reflect the spatial variation law of the UHI effect, and the annual change rate of the UHI effect was calculated by the least square method. Assuming: i represents the serial number of the year; GBC represents the green building coverage index in the i -th year; m represents the total number of study years; ω_{SL} represents the change rate of green building coverage index in the study period, then the calculation formula of ω_{SL} can be expressed as:

$$\omega_{SL} = m \times \sum_{i=1}^m (i \times NDVI_i) - \left(\sum_{i=1}^m i \times \sum_{i=1}^m NDVI_i \right) / \left(m \times \sum_{i=1}^m (i^2) - \left(\sum_{i=1}^m i \right)^2 \right) \quad (17)$$

If the value of ω_{SL} is greater than 0, it means that the distribution of green building pixels is developing towards to a good direction; if the value of ω_{SL} is less than 0, it means that the distribution of green building pixels is getting worse and has a risk of degradation.

In this paper, the correlations between each pair of factors were analyzed, including the green building coverage index and air temperature, and the green building coverage index and precipitation. Assuming: e_{uv} represents the correlation coefficient between factor u and factor v ; u^* and v^* represent the average values of the samples of the two factors, then there is:

$$e_{ab} = \frac{\sum_{i=1}^m (u_i - u^*)(v_i - v^*)}{\sqrt{\sum_{i=1}^m (u_i - u^*)^2} \sqrt{\sum_{i=1}^m (v_i - v^*)^2}} \quad (18)$$

The value range of e is $[-1, 1]$. When e is greater than 0, the two factors are positively correlated. When e is less than 0, the two factors are negatively correlated. When e is equal to 0, it means that there isn't a linear relationship between the two. If the value of $|e|$ is 1, it means the two factors are perfectly linearly correlated.

During the study period, ordinary buildings can be transformed into green buildings through renovation. This paper employed a land utilization transition matrix to measure the change features of the coverage of ordinary buildings. Assuming i represents the area and feature of the land utilization type of ordinary buildings in the beginning of the study period; j represents the land utilization type of ordinary buildings in the end of the study period; m represents the total number of land utilization types, then Formula 19 shows the expression of the land utilization transition matrix:

$$r_{ij} = \begin{pmatrix} r_{11} & \cdots & r_{1m} \\ \vdots & \ddots & \vdots \\ r_{m1} & \cdots & r_{mm} \end{pmatrix} \quad (19)$$

In this paper, the net change rate of land utilization type was used to measure the area change rate of the land utilization type of ordinary buildings and the future trend. Assuming: NC represents the net change rate of the land utilization type of ordinary buildings; V_x represents the area of the land utilization type of ordinary buildings in the beginning of the study period; V_y represents the area of the land utilization type of ordinary buildings in the end of the study period; p represents the number of study years, then there is:

$$NC = \frac{V_y - V_x}{V_x} \times \frac{1}{p} \times 100\% \quad (20)$$

In this paper, the land area change rate of green buildings was used to measure the change trend and intensity degree of the specific land utilization type of green buildings within the study period. Assuming IA represents the initial area of the land utilization type of green buildings in the study period; FA represents the final area of the land utilization type of green buildings, then there is:

$$ACR = \frac{FA_j - IA_j}{IA_j} \times 100\% \quad (21)$$

In this paper, the change intensity index of green buildings was used to study the changes in the area of the specific land

utilization type of green buildings in the study period. Assuming RA represents the area of urban earth surface; m represents the number of land utilization types; ZA represents the total area of the land utilization type of ordinary buildings that has transformed into the land utilization type of green buildings; correspondingly, TA represents the total area of the land utilization type of green buildings that has transformed into the land utilization type of ordinary buildings, then there is:

$$GBCI = \frac{\sum_{j=1}^m (ZA_j + TA_j)}{2 \times RA} \times 100\% \quad (22)$$

4. EXPERIMENTAL RESULTS AND ANALYSIS

Table 2 shows the statistical results of the average values of the UHI effect. As can be seen from the data, the UHI index of more than 20% of the green building pixels was less than -5°C , and the UHI index of more than 40% of the green building pixels was between -5°C and 0°C . Table 3 gives the change rate of the UHI effect in the study area. In the four sub-areas of the study area, the average slope of the UHI effect in the core area was greater than 0, and the standard deviation was relatively large, indicating that the difference between green building pixels and ordinary building pixels in this area was large.

Table 2. Average values of the UHI effect

Area code	A	B	C	D	The overall area
Less than -5°C	6.052%	4.918%	5.648%	5.211%	6.381%
$[-5^\circ\text{C}, 0^\circ\text{C}]$	26.841%	36.174%	33.415%	28.995%	30.628%
$[0^\circ\text{C}, 5^\circ\text{C}]$	41.928%	45.627%	43.629%	49.567%	43.914%
Greater than 5°C	25.179%	13.281%	17.308%	16.227%	19.077%

Table 3. Change rate of the UHI effect in the study area

Area code	A				B			
	A ₁	A ₂	A ₃	A ₄	B ₁	B ₂	B ₃	B ₄
Sub-area								
Minimum	-0.326	-0.384	-0.516	-0.492	-0.382	-0.437	-0.374	-0.395
Maximum	0.481	0.539	0.491	0.562	0.392	0.348	0.329	0.472
Mean	0.017	0.035	-0.042	-0.019	-0.092	-0.084	-0.017	0.028
Standard deviation	0.048	0.062	0.049	0.082	0.097	0.068	0.053	0.092
Area code	C				D			
	C ₁	C ₂	C ₃	C ₄	D ₁	D ₂	D ₃	D ₄
Sub-area								
Minimum	-0.216	-0.375	-0.438	-0.395	-0.279	-0.298	-0.339	-0.324
Maximum	0.325	0.592	0.438	0.286	0.317	0.371	0.284	0.416
Mean	0.039	-0.037	-0.074	0.039	-0.084	-0.088	-0.032	0.053
Standard deviation	0.081	0.063	0.076	0.084	0.014	0.025	0.044	0.049

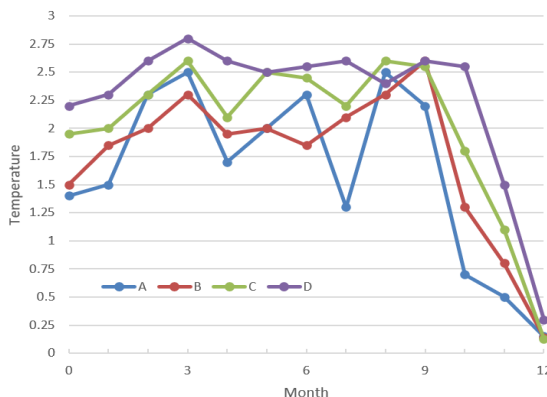


Figure 2. Changes of the UHI effect in the study area

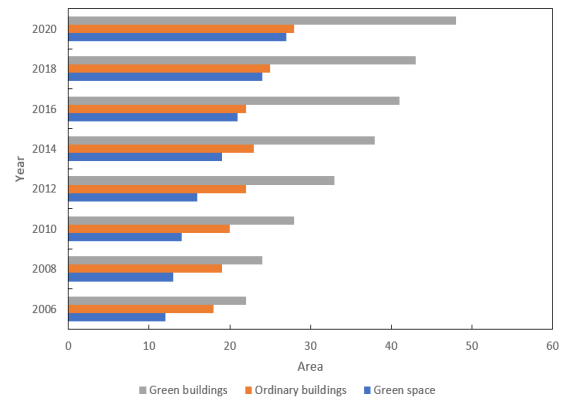


Figure 3. Changes in the area of different land utilization types

The change trends of the UHI effect in the four sub-areas are shown in Figure 2. As can be seen from the figure, the value the UHI index of the study area reached the minimum of about 0.14°C between January and March. Between September to December, the value of the UHI index showed an obvious downward trend, and the temperature drop was about 2.5°C. The change trend of the UHI index between March and June was completely opposite to that between September and December. The value of the UHI index between June and September was higher than that of other seasons. The value of the UHI index of sub-area D was the highest among all sub-areas, and the value of the UHI index of sub-area A was the lowest.

The data of the net change rate of land utilization types from 2006 to 2020 were analyzed to determine the coverage of green buildings and the area of each land utilization type such as ordinary buildings and green space. Figure 3 shows the changes in the area of different land utilization types. On the whole, the area of ordinary building in the study period increased first and decreased later. Between 2006 and 2020, the area of green building and the area of green space both showed a gradual increase trend, the net change rates of the two reached 50.58% and 55.67%, respectively.

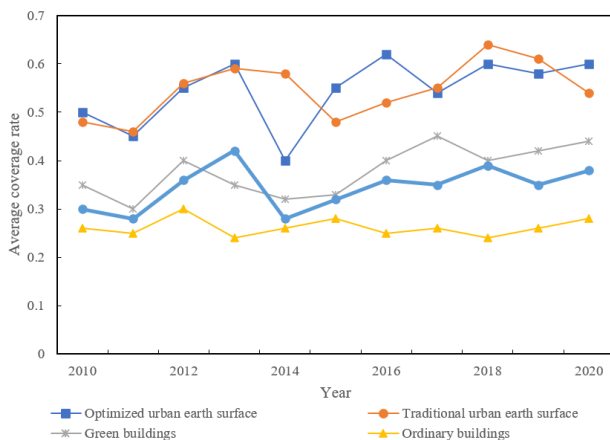


Figure 4. Changes in the coverage rate of different land utilization types

As shown in Figure 4 above, during 2010 and 2020, from large to small, the average coverage rate of the study area was: optimized urban earth surface > traditional urban earth surface > green buildings > ordinary buildings > green space, and all of them showed a slow increase trend, wherein the average coverage rate of green buildings was 0.412, the average coverage rate of ordinary buildings was 0.378, the average coverage rate of green space was 0.214, and the average coverage rates of optimized urban earth surface and traditional urban earth surface were 0.565 and 0.537, respectively. Viewing from the change trend, the coverage rates of traditional urban earth surface, optimized urban earth surface, green space, ordinary buildings, and green buildings all showed an improvement, and the improvement of the coverage rate of green buildings was the most significant.

5. CONCLUSION

This paper studied the optimization of the distribution of green buildings based on the UHI effect. At first, it adopted a high-precision radiative transfer model to invert the

temperature of earth surface in cities and accurately calculate the UHI effect. Then, the paper analyzed the changes in the UHI effect caused by the optimization of the distribution of green buildings and the response of human activities, and used the time variation law of the single pixels of green buildings to reflect the spatial variation law of the UHI effect. At last, this paper counted the average values and changes of the UHI index of the study area, verified the large difference between green building pixels and ordinary building pixels in the study area, gave the changes in the UHI effect in the study area, the changes in the area and coverage rate of various land utilization types in the study area, and gave the optimization results of green building distribution based on an analysis of the UHI effect. The experimental results showed that, the coverage rates of traditional urban earth surface, optimized urban earth surface, green space, ordinary buildings, and green buildings all exhibited an improvement trend, and the improvement of the coverage rate of green buildings was the most obvious.

ACKNOWLEDGMENT

"Research on land ecological security utilization and farmers' livelihood response." The innovation training program for college students of Hunan Agricultural University (Grant No.: s202010537080).

REFERENCES

- [1] Palme, M., Lobato, A., Carrasco, C. (2016). Quantitative analysis of factors contributing to urban heat island effect in cities of latin-american Pacific coast. *Procedia Engineering*, 169: 199-206. <https://doi.org/10.1016/j.proeng.2016.10.024>
- [2] Subhashini, S., Thirumaran, K., Saravanan, V., Alaguraja, R.A. (2016). A Comparative analysis of land surface retrieval methods using landsat 7 and 8 Data to study urban heat island effect in madurai. *International Journal of Earth Sciences and Engineering*, 9(4): 1397-1404.
- [3] Yin, C., Yuan, M., Lu, Y., Huang, Y., Liu, Y. (2018). Effects of urban form on the urban heat island effect based on spatial regression model. *Science of the Total Environment*, 634: 696-704. <https://doi.org/10.1016/j.scitotenv.2018.03.350>
- [4] Yang, Y.K., Kang, I.S., Chung, M.H., Kim, S., Park, J. C. (2017). Effect of PCM cool roof system on the reduction in urban heat island phenomenon. *Building and Environment*, 122: 411-421. <https://doi.org/10.1016/j.buildenv.2017.06.015>
- [5] Chen, J., Wang, H., Zhu, H. (2017). Analytical approach for evaluating temperature field of thermal modified asphalt pavement and urban heat island effect. *Applied Thermal Engineering*, 113: 739-748. <https://doi.org/10.1016/j.applthermaleng.2016.11.080>
- [6] Theophilou, M.K., Serghides, D. (2015). Estimating the characteristics of the Urban Heat Island Effect in Nicosia, Cyprus, using multiyear urban and rural climatic data and analysis. *Energy and Buildings*, 108: 137-144. <https://doi.org/10.1016/j.enbuild.2015.08.034>
- [7] Chapman, S., Thatcher, M., Salazar, A., Watson, J.E., McAlpine, C.A. (2018). The effect of urban density and

- vegetation cover on the heat island of a subtropical city. *Journal of Applied Meteorology and Climatology*, 57(11): 2531-2550. <https://doi.org/10.1175/JAMC-D-17-0316.1>
- [8] Shi, Y., Katzschner, L., Ng, E. (2018). Modelling the fine-scale spatiotemporal pattern of urban heat island effect using land use regression approach in a megacity. *Science of the Total Environment*, 618: 891-904.
- [9] Mathew, A., Khandelwal, S., Kaul, N. (2016). Spatial and temporal variations of urban heat island effect and the effect of percentage impervious surface area and elevation on land surface temperature: Study of Chandigarh city, India. *Sustainable Cities and Society*, 26: 264-277. <https://doi.org/10.1016/j.scs.2016.06.018>
- [10] Li, Y.K., Chao, J.P., Kuang, G.X. (2015). Dynamic and thermodynamic analysis of the urban heat island effect and aerosol concentration. *Chinese Journal of Geophysics*, 58(3): 729-740. <https://doi.org/10.6038/cjg20150303>
- [11] Gagliano, A., Nocera, F., Aneli, S. (2017). Computational fluid dynamics analysis for evaluating the urban heat island effects. *Energy Procedia*, 134: 508-517. <https://doi.org/10.1016/j.egypro.2017.09.557>
- [12] Tu, L., Qin, Z., Li, W., Geng, J., Yang, L., Zhao, S.H., Zhan, W.F., Wang, F. (2016). Surface urban heat island effect and its relationship with urban expansion in Nanjing, China. *Journal of Applied Remote Sensing*, 10(2): 026037. <https://doi.org/10.1117/1.JRS.10.026037>
- [13] Fang, G. (2015). Prediction and analysis of urban heat island effect in dangshan by remote sensing. *International Journal on Smart Sensing & Intelligent Systems*, 8(4): 2195-2211. <https://doi.org/10.21307/ijssis-2017-849>
- [14] Wang, S.Y., Zhu, Q.Y., Duan, Y.N., Shang, P.D. (2014). Unidirectional heat-transfer asphalt pavement for mitigating the urban heat island effect. *Journal of Materials in Civil Engineering*, 26(5): 812-821. [https://doi.org/10.1061/\(ASCE\)MT.1943-5533.0000872](https://doi.org/10.1061/(ASCE)MT.1943-5533.0000872)
- [15] Feyisa, G.L., Dons, K., Meilby, H. (2014). Efficiency of parks in mitigating urban heat island effect: An example from Addis Ababa. *Landscape and Urban Planning*, 123: 87-95. <https://doi.org/10.1016/j.landurbplan.2013.12.008>
- [16] Čeplová, N., Kalusová, V., Lososová, Z. (2017). Effects of settlement size, urban heat island and habitat type on urban plant biodiversity. *Landscape and Urban Planning*, 159: 15-22. <https://doi.org/10.1016/j.landurbplan.2016.11.004>
- [17] Liu, K., Su, H., Zhang, L., Yang, H., Zhang, R., Li, X. (2015). Analysis of the urban heat island effect in Shijiazhuang, China using satellite and airborne data. *Remote Sensing*, 7(4): 4804-4833. <https://doi.org/10.3390/rs70404804>
- [18] Zhang, Y., Murray, A.T., Turner Ii, B.L. (2017). Optimizing green space locations to reduce daytime and nighttime urban heat island effects in Phoenix, Arizona. *Landscape and Urban Planning*, 165: 162-171. <https://doi.org/10.1016/j.landurbplan.2017.04.009>
- [19] He, Y., Kvan, T., Liu, M., Li, B. (2018). How green building rating systems affect designing green. *Building and Environment*, 133: 19-31. <https://doi.org/10.1016/j.buildenv.2018.02.007>
- [20] Ding, Z., Fan, Z., Tam, V.W., Bian, Y., Li, S., Illankoon, I.C.S., Moon, S. (2018). Green building evaluation system implementation. *Building and Environment*, 133: 32-40. <https://doi.org/10.1016/j.buildenv.2018.02.012>
- [21] Fan, Y., Xia, X. (2018). Energy-efficiency building retrofit planning for green building compliance. *Building and Environment*, 136: 312-321. <https://doi.org/10.1016/j.buildenv.2018.03.044>
- [22] Vyas, G.S., Jha, K.N. (2018). What does it cost to convert a non-rated building into a green building? *Sustainable Cities and Society*, 36: 107-115. <https://doi.org/10.1016/j.scs.2017.09.023>
- [23] Gao, C., Zhang, W., Tang, J. (2016). Building elastic hybrid green wireless networks. *IEEE Internet of Things Journal*, 4(6): 2028-2037. <https://doi.org/10.1109/JIOT.2016.2642823>
- [24] Yao, M. (2017). Green design of public building and evaluation. *Agro Food Industry Hi-Tech*, 28(1): 26-28.
- [25] Lai, X., Lyu, Y., Wang, F. (2017). Fuzzy multilevel index comprehensive evaluation model of green building. *Boletín Técnico*, 55(16): 366-373.
- [26] Chiang Hsieh, L.H., Noonan, D. (2017). Strategic behavior in certifying green buildings: an inquiry of the non-building performance value. *Environmental Management*, 60(2): 231-242. <https://doi.org/10.1007/s00267-017-0869-5>
- [27] Reychar, I., Maskil Leitan, R., McHaney, R. (2017). Sociocultural sustainability in green building information modeling. *Clean Technologies and Environmental Policy*, 19(9): 2245-2254. <https://doi.org/10.1007/s10098-017-1409-y>
- [28] Susca, T., Zanghirella, F., Colasuonno, L., Del Fatto, V. (2022). Effect of green wall installation on urban heat island and building energy use: A climate-informed systematic literature review. *Renewable and Sustainable Energy Reviews*, 159: 112100. <https://doi.org/10.1016/j.rser.2022.112100>
- [29] He, B.J. (2019). Towards the next generation of green building for urban heat island mitigation: Zero UHI impact building. *Sustainable Cities and Society*, 50: 101647. <https://doi.org/10.1016/j.scs.2019.101647>
- [30] Sun, C.Y., Lin, Y.J., Sung, W.P., Ou, W.S., Lu, K.M. (2012). Green roof as a green material of building in mitigating heat island effect in Taipei city. In *Applied Mechanics and Materials*, 193: 368-371. <https://doi.org/10.4028/www.scientific.net/AMM.193-194.368>
- [31] Wang, K., Mao, W. (2021). Simulation of vertical temperature distribution in green building space based on the niche genetic algorithm. In *2021 IEEE International Conference on Industrial Application of Artificial Intelligence (IAAI)*, pp. 123-130. <https://doi.org/10.1109/IAAI54625.2021.9699944>
- [32] Tong, Z. (2016). A genetic algorithm approach to optimizing the distribution of buildings in urban green space. *Automation in Construction*, 72: 46-51. <https://doi.org/10.1016/j.autcon.2016.10.001>